Wave propagation modeling in coastal engineering
Modélisation de la houle en ingénierie côtière

PHILIP L.-F. LIU, *School of Civil and Environmental Engineering, Cornell University, Ithaca, NY, USA*

INIGO J. LOSADA, *Ocean and Coastal Research Group, Universidad de Cantabria, Santander, Spain*

ABSTRACT
In this paper we review various numerical models for calculating wave propagations from deep water to surf zone, including wave breaking. The limitations and the approximations for each model are briefly discussed. The main focus of the discussions is on the unified depth-integrated model, which can describe fully nonlinear and weakly dispersive waves, and the Reynolds Averaged Navier-Stokes equations model, which can calculate breaking waves and associated turbulence. Several applications of various models are also presented.

RÉSUMÉ
Dans cet article nous passons en revue les différents modèles permettant de calculer les propagations de houle depuis les eaux profondes jusqu'aux zones de surf, incluant le déferlement. Les limitations et approximations de chaque modèle sont brièvement discutées. Les discussions portent principalement sur le modèle unifié moyenné en profondeur, qui peut décrire les houles complètement non linéaires et faiblement dispersives, et le modèle des équations de Navier-Stokes en moyenne de Reynolds, qui peut calculer la houle déferlante et la turbulence associée. Plusieurs applications des différents modèles sont également présentées.

1. Introduction

Every coastal or ocean engineering study such as a beach nourishment project or a harbor design planning, requires the information of wave conditions in the region of interest. Usually, wave characteristics are collected offshore and it is necessary to transfer these offshore data on wave heights and wave propagation direction to the project site. The increasing demands for accurate design wave conditions and for input data for the investigation of sediment transport and surf zone circulation have resulted in significant advancement of wave transformation models during the last two decades (Mei and Liu 1993).

When wind waves are generated by a distance storm, they usually consist of a wide range of wave frequencies. The wave component with a higher wave frequency propagates at a slower speed than those with lower wave frequencies. As they propagate across the continental shelf towards the coast, long waves lead the wave group and are followed by short waves. In the deep water, wind generated waves are not affected by the bathymetry. Upon entering shoaling waters, however, they are either refracted by bathymetry or current, or diffracted around abrupt bathymetric features such as submarine ridges or canyons. A part of wave energy is reflected back to the deep sea. Continuing their shoreward propagation, waves lose some of their energy through dissipation near the bottom. Nevertheless, each wave profile becomes steeper with increasing wave amplitude and decreasing wavelength. Because the wave speed is proportional to the square root of the water depth in very shallow water, the front face of a wave moves at a slower speed than the wave crest, causing the overturning motion of the wave crest. Such an overturning motion usually creates a jet of water, which falls near the base of the wave and generates a large splash. Turbulence associated with breaking waves is responsible not only for the energy dissipation but also for the sediment movement in the surfzone.

In the early 1960's the wave ray tracing method was a common tool for estimating wave characteristics at a design site. Today, powerful computers have provided coastal engineers with the opportunity to employ more sophisticated numerical models for wave environment assessment. However, these numerical models are still based on simplified governing equations, boundary conditions and numerical schemes, imposing different restrictions to practical applications. The computational effort required for solving a wave propagation problem exactly by taking all physical processes, which involve many different temporal and spatial scales, into account is still too large.

To date, two basic kinds of numerical wave models can be distinguished: phase-resolving models, which are based on vertically integrated, time-dependent mass and momentum balance equations, and phase-averaged models, which are based on a spectral energy balance equation. The application of phase-resolving models, which require 10 ~ 100 time steps for each wave period, is still limited to relatively small areas, O (1 ~ 10 km), while phase-averaged models are more relax in the spatial resolution and can be used in much larger regions. Moreover, none of the existing models, phase-resolving or not, considers all physical processes involved.

The more recent research efforts have been focused on the development of unified phase-resolving models, which can describe transient fully nonlinear wave propagation from deep water to shallow water over a large area. In the mean time, significant progress has also been made in simulating the wave-breaking process by solving the Reynolds Averaged Navier Stokes (RANS) equations with a turbulence closure model. These RANS models have also been employed in the studies of wave and structure interactions.

The purpose of this paper is to provide a short summary of the

Revision received May 20, 2002. Open for discussion till August 31, 2002.

evolution of phase-resolving wave propagation models during the last two decades, especially focusing on the most recent advances regarding the development of unified models and the simulation of the wave breaking process.

2. Depth-integrated Models

In principle, water wave motions without breaking can be modeled by the Navier-Stokes equations for incompressible Newtonian fluids, which represent the conservation of mass and momentum. Free surface boundary conditions, ensuring the continuity of stress tensor across the free surface and the free surface is a material surface, are necessary in determining the free surface location. Both the Navier-Stokes equations and the free surface boundary conditions are nonlinear. Consequently, even when the viscous and turbulence effects can be ignored, the computational effort required for solving a truly three-dimensional wave propagation problem, which has a horizontal length scale of over hundreds or more wavelengths, is too large to be employed in engineering design practice at this time.

2.1 Ray approximation

Efforts for reducing the computational time are necessary and have been sought by reducing the dimension of the computational domain. Moreover, continuing efforts have been made to construct a unified model that can propagate wave from deep water into shallow water, even into the surf zone. The forerunner of this kind of effort is the ***ray approximation*** for ***infinitesimal waves*** propagating over bathymetry that varies slowly over horizontal distances much longer than local wavelength. In this approximation, one first finds wave rays by adopting the geometrical optic theory, which defines the wave ray as a curve tangential to the wave number vector. One then calculates the spatial variation of the wave envelope along the rays by invoking the principle of conservation of energy. Numerical discretization can be done in steps along a ray not necessarily small in comparison with a typical wavelength. Since the ray approximation does not allow wave energy flux across a wave ray, it fails near the caustics or the focal regions, where neighboring wave rays intersect; diffract and possibly nonlinearity are important. While ad hoc numerical methods for local remedies are available, it is not always convenient to implement them in practice.

2.2 Mild-slope equation

Within the framework of linear wave theory, an improvement to the ray approximation was first suggested by Eckart (1952) and was later rederived by Berkhoff (1972, 1976), who proposed a two-dimensional theory that can deal with large regions of refraction and diffraction. The underlying assumption of the theory is that evanescent modes are not important for waves propagating over a slowly varying bathymetry, except in the immediate vicinity of a three-dimensional obstacle. For a monochromatic wave with frequency ω and free surface displacement η, it is reasonable to express the velocity potential, which formally represents the propagating mode only, as:

$$\phi = \frac{-ig\eta}{\omega}\frac{\cosh k(z+h)}{\cosh kh}e^{-i\omega t} \tag{1}$$

where $k(x, y)$ and $h(x, y)$ vary slowly in the horizontal directions, x and y, according to the linear frequency dispersion relation

$$\omega^2 = gk\tanh kh \tag{2}$$

and g is the gravitational acceleration. By a perturbation argument Smith and Sprinks (1975) have also shown that the free surface displacement η must satisfy the following equation:

$$\nabla\cdot(CC_g\nabla\eta)+\frac{\omega^2}{g}\eta = 0, \tag{3}$$

where

$$C = \frac{\omega}{k}, C_g = \frac{d\omega}{dk} = \frac{C}{2}\left(1+\frac{2kh}{\sinh 2kh}\right), \tag{4}$$

are the local phase and group velocities of a plane progressive wave. The elliptic-type partial differential equation, (3), is asymptotically valid for sufficiently small δ (= $|\nabla h|/kh$ to leading order) and is known as the ***mild-slope equation***. An indication of its versatility can be seen in two limits. For long waves in shallow water the limit of (3) at $kh<<1$ reduces to the well-known linear shallow-water equation that is valid even if $\delta=O(1)$. On the other hand, if the depth is a constant or for short waves in deep water ($kh>>1$), (3) reduces to the Helmholtz equation where k satisfies the dispersion relation (2). Both limits can be used to calculate diffraction legitimately. Thus, the mild slope-equation should be a good interpolation for all kh and is suitable for propagating waves from deep water to shallow water as long as the linearization is acceptable. A similar mild-slope equation for waves propagating over gradually varying currents has also been derived (*e.g.* Liu, 1990).

The key reason for the success of the mild-slope equation in modeling wave propagation from deep water to shallow water is because the vertical profile of the velocity, (1), is prescribed "correctly" according to the linear wave theory. The mild-slope equation can be applied to a wave system with multiple wave components as long as the system is linear and these components do not interact with each other.

2.3 Parabolic approximation

In applying the mild-slope equation to a large region in coastal zone, one encounters the difficulty of specifying boundary conditions along the shoreline, which are essential for solving the elliptic-type mild-slope equation. The difficulty arises because the location of the breaker cannot be determined *a priori*. A remedy to this problem is to apply the ***parabolic approximation*** to the mild-slope equation (Kirby and Dalrymple 1983; Tsay and Liu 1982). For essentially forward propagation problems, the so-called parabolic approximation expands the validity of the ray

theory by allowing wave energy "diffuse" across the wave "ray". Therefore, the effects of diffraction have been approximately included in the parabolic approximation. For instance, in the mild-slope equation, (3), the free surface displacement η can be approximated as a wave propagating in the x-direction with an amplitude that varies in both horizontal directions. Thus,

$$\eta = \xi(x,y)e^{ik_o x} \tag{5}$$

where k_0 is a reference constant wave number. The parabolic approximation assumes that the amplitude function *A varies much faster in the y-direction than the x-direction,* $\partial^2\xi/\partial y^2 \gg \partial^2\xi/\partial x^2$. Substituting (5) into (3) and adopting the parabolic approximation yield the following parabolic equation

$$\frac{\partial^2\xi}{\partial y^2} + \left(2ik_0 + \frac{1}{CC_g}\frac{\partial CC_g}{\partial x}\right)\frac{\partial\xi}{\partial x} + \frac{1}{CC_g}\frac{\partial CC_g}{\partial y}\frac{\partial\xi}{\partial y} + \left(\frac{\omega^2}{g} - k_0^2 + \frac{ik_0}{CC_g}\frac{\partial CC_g}{\partial x}\right)\xi = 0 \tag{6}$$

Although the parabolic approximation has been used primarily for forward propagation, adopting an iterative procedure can also include weakly backward propagation (*e.g.*, Liu and Tsay 1983; Chen and Liu 1994).

We reiterated here that the original parabolic approximation is based on the monochromatic linear wave theory. The extension of the mild-slope equation and the parabolic approximations to transient waves must be exercised with care.

The practical application of wave transformation usually requires the simulation of directional random waves. Because of the linear characteristics of the mild-slope equation and the parabolic approximation, the principle of superposition of different wave frequency components can be applied. In general, parabolic models for spectral wave conditions require inputs of the incoming directional random sea at the offshore boundary. The two-dimensional input spectra are discretized into a finite number of frequency and direction wave components. Using the parabolic equation, the evolution of the amplitudes of all the wave components is computed simultaneously. Based on the calculations for all components, and assuming a Rayleigh distribution, statistical quantities such as the significant wave height H_s can be calculated at every grid point. In figure1 a snap shot of the free surface elevation is shown; it is based on the numerical simulations of wave propagation near Gijon Harbor (Spain), using a parabolic approximation of the mild slope equation for spectral wave conditions. Further demonstrations of the capabilities of wave propagation modeling based on the parabolic approximation of the mild-slope equation including wave breaking will be shown later in this paper.

2.4 Stokes waves

For finite amplitude waves, the usual linearization assumptions, which require that

Fig. 1 A snap shot of the free surface elevation based on the numerical simulations of wave propagation near Gijon Harbor (Spain), using a parabolic approximation of the mild slope equation for spectral wave conditions. (GIOC, 2000).

$$kA \ll 1 \text{ everywhere and } A/h \ll 1 \text{ in shallow water } (kh \ll 1) \tag{7}$$

might become invalid. A more relevant theory in the deep water and intermediate water is perhaps the ***higher-order Stokes wave theories*** that take the effects of finite wave amplitude into consideration in the perturbation sense. The finiteness of the wave amplitude has direct effect on the frequency dispersion and consequently the phase speed. For instance, for the second-order Stokes wave, the nonlinear dispersion relation has the following form:

$$\omega^2 = gk\tanh kh + \kappa A^2 + \cdots \tag{8}$$

where

$$\kappa = \frac{k^4C^2}{8\sinh^4 kh}\left(8 + \cosh 4kh - 2\tanh^2 kh\right) \tag{9}$$

and A denotes the wave amplitude. Equation (8) can be viewed as a power series in terms of the small parameter $kA \ll 1$. The corresponding nonlinear mild-slope equation and its parabolic approximation have been derived and reported by Kirby and Dalrymple (1983) and Liu and Tsay (1984). However, one must exercise caution in extending the nonlinear Stokes wave theory into the shallow water; additional condition needs to be satisfied. In the limit of $kh \ll 1$ the nonlinear dispersion relation can be approximated as:

$$\omega^2 = ghk^2\left(1 + \frac{9}{8}\frac{A/h}{k^2h^2}\frac{A}{h} + \cdots\right) \tag{10}$$

To ensure the series converges for $A/h \ll 1$, one must make sure that the coefficient of the second term in the series is of order one or smaller, *i.e.,*

$$U_r = O\left(\frac{A/h}{(kh)^2}\right) \le O(1) \tag{11}$$

which is also called ***Ursell parameter***. The condition (11), requiring the Ursell parameter to be of order one or smaller in the shallow water region, is very difficult to fulfill in practice. According to the linear theory, in shallow water the wave amplitude, A, grows proportionally to $h^{-1/4}$ and kh decreases as $\sqrt{h}$. Therefore, the Ursell parameter will grow according to $h^{-9/4}$ as the water depth decreases and will certainly exceed order one at certain depth. One can conclude that nonlinear Stokes wave theory is not applicable in the shallow water and alternative model equations must be found.

2.5 Boussinesq approximation

Assuming that both nonlinearity and frequency dispersion are weak and are in the same order of magnitude, Peregrine (1967) derived the ***standard Boussinesq equations*** for variable depth.

$$\eta_t + \nabla\cdot\left[(\eta+h)\bar{\boldsymbol{u}}\right] = 0 \tag{12}$$

$$\bar{\boldsymbol{u}}_t + \frac{1}{2}\nabla|\bar{\boldsymbol{u}}|^2 + g\nabla\eta + \left\{\frac{h^2}{6}\nabla\left(\nabla\cdot\bar{\boldsymbol{u}}_t\right) - \frac{h}{2}\nabla\left(\nabla\cdot\left(h\bar{\boldsymbol{u}}_t\right)\right)\right\} = 0 \tag{13}$$

in which $\bar{\boldsymbol{u}}$ is the depth-averaged velocity, η the free surface displacement; h the still water depth, $\nabla = (\partial/\partial x, \partial/\partial y)$ the horizontal gradient operator, g the gravitational acceleration; and subscript t the partial derivative with respect to time. Boussinesq equations can be recast into similar equations in terms of either the velocity on the bottom or the velocity on the free surface. While the dispersion relationship and the wave speed associated with these equations differ slightly, the order of magnitude of accuracy of these equations remains the same. Numerical results based on the standard Boussinesq equations or the equivalent formulations have been shown to give predictions that compared quite well with field data (Elgar and Guza 1985) and laboratory data (Goring 1978, Liu *et al*. 1985).

Because it is required that both frequency dispersion and nonlinear effects are weak, the standard Boussinesq equations are not applicable to very shallow water depth, where the nonlinearity becomes more important than the frequency dispersion, and to the deep water depth, where the frequency dispersion is of order one. The standard Boussinesq equations written in terms of the depth-averaged velocity break down when the depth is greater than one-fifth of the equivalent deep-water wavelength. For many engineering applications, where the incident wave energy spectrum consists of many frequency components, a lesser depth restriction is desirable. Furthermore, when the Boussinesq equations are solved numerically, high frequency oscillations with wavelengths related to the grid size could cause instability. To extend the applications to shorter waves (or deeper water depth) many modified forms of Boussinesq-type equations have been introduced (*e.g.,* Madsen *et al.* 1991, Nwogu 1993, Chen and Liu, 1995). Although the methods of derivation are different, the resulting dispersion relations of the linear components of these modified Boussinesq equations are similar, and may be viewed as a slight modification of the (2,2) Pade approximation of the full dispersion relation for linear water wave (Witting 1984). Following Nwogu's approach (1993), the depth-integrated continuity equation and momentum equations can be expressed in terms of the free surface displacement η and $\boldsymbol{u}_\alpha$, the horizontal velocity vector at the water depth $z=z_\alpha$, can be expressed as:

$$\eta_t + \nabla\cdot\left[(\eta+h)\boldsymbol{u}_\alpha\right] + \nabla\cdot\left\{\left(\frac{z_\alpha^2}{2} - \frac{h^2}{6}\right)h\nabla\left(\nabla\cdot\boldsymbol{u}_\alpha\right) + \left(z_\alpha + \frac{h}{2}\right)h\nabla\left(\nabla\cdot h\boldsymbol{u}_\alpha\right)\right\} = 0 \tag{14}$$

$$\boldsymbol{u}_{\alpha t} + \frac{1}{2}\nabla|\boldsymbol{u}_\alpha|^2 + g\nabla\eta + z_\alpha\left\{\tfrac{1}{2}z_\alpha\nabla\left(\nabla\cdot\boldsymbol{u}_{\alpha t}\right) + \nabla\left(\nabla\cdot\left(h\boldsymbol{u}_{\alpha t}\right)\right)\right\} = 0 \tag{15}$$

It has been demonstrated that with optimal choice of, z_α=-0.531h the ***modified Boussinesq equations*** are able to simulate wave propagation from intermediate water depth (water depth to wavelength ratio is about 0.5) to shallow water including the wave-current interaction (Chen *et al*. 1998). It should be also pointed out that the convective acceleration in the momentum equation (13) and (15) has been written in the conservative form. One could replace them by the non-conservative form, *i.e.* $\bar{\boldsymbol{u}}\cdot\nabla\bar{\boldsymbol{u}}$ and $\boldsymbol{u}_\alpha\cdot\nabla\boldsymbol{u}_\alpha$, respectively, without changing the order of magnitude of accuracy of the model equations.

2.6 Highly nonlinear and dispersive models

Despite of the success of the modified Boussinesq equations in intermediate water depth, these equations are still restricted to weakly nonlinearity. As waves approach shore, wave height increases due to shoaling and wave breaks on most of gentle natural beaches. The wave-height to water depth ratios associated with this physical process become too high for the Boussinesq approximation. The appropriate model equation for the leading order solution should be the nonlinear shallow water equation. Of course this restriction can be readily removed by eliminating the weak nonlinearity assumption (*e.g.,* Liu 1994, Wei *et al*. 1995). Strictly speaking, these fully nonlinear equations can no longer be called Boussinesq-type equations since the nonlinearity is not in balance with the frequency dispersion, which violates the spirit of the original Boussinesq assumption.

The fully nonlinear but weakly dispersive wave equations have been presented by many researchers and can be written as (*e.g*., Liu, 1994):

$$\eta_t + \nabla\cdot\left\{(h+\eta)\left[\boldsymbol{u}_\alpha + \left(z_\alpha + \tfrac{1}{2}(h-\eta)\right)\nabla\left(\nabla\cdot(h\boldsymbol{u}_\alpha)\right) + \left(\tfrac{1}{2}z_\alpha^2 - \tfrac{1}{6}\left(h^2 - h\eta + \eta^2\right)\right)\nabla\left(\nabla\cdot\boldsymbol{u}_\alpha\right)\right]\right\} = 0 \tag{16}$$

$$\begin{aligned}\boldsymbol{u}_{\alpha t} &+ \frac{1}{2}\nabla|\boldsymbol{u}_\alpha|^2 + g\nabla\eta \\ &+ z_\alpha\left\{\tfrac{1}{2}z_\alpha\nabla\left(\nabla\cdot\boldsymbol{u}_{\alpha t}\right) + \nabla\left(\nabla\cdot(h\boldsymbol{u}_{\alpha t})\right)\right\} \\ &+ \nabla\left\{\begin{array}{l}\tfrac{1}{2}\left(z_\alpha^2 - \eta^2\right)\left(\boldsymbol{u}_\alpha\cdot\nabla\right)\left(\nabla\cdot\boldsymbol{u}_\alpha\right) \\ + \tfrac{1}{2}\left[\nabla\cdot(h\boldsymbol{u}_\alpha) + \eta\nabla\cdot\boldsymbol{u}_\alpha\right]^2\end{array}\right\} \\ &+ \nabla\left\{\begin{array}{l}\left(z_\alpha - \eta\right)\left(\boldsymbol{u}_\alpha\cdot\nabla\right)\left(\nabla\cdot(h\boldsymbol{u}_\alpha)\right) \\ - \eta\left[\tfrac{1}{2}\eta\nabla\cdot\boldsymbol{u}_{\alpha t} + \nabla\cdot(h\boldsymbol{u}_{\alpha t})\right]\end{array}\right\} = 0\end{aligned} \tag{17}$$

These equations are the statements of conservation of mass and momentum respectively. They are derived without making any approximation on the nonlinearity. Therefore, if one were to replace the conservative form of the inertia term, $\frac{1}{2}\nabla|\boldsymbol{u}_\alpha|^2$, by $\boldsymbol{u}_\alpha\cdot\nabla\boldsymbol{u}_\alpha$ in the momentum equation, (17), additional higher order terms must be added to maintain the order of magnitude in accuracy. It is straightforward to show that the conventional Boussinesq equations, (12) and (13), and the modified Boussinesq equations, (14) and (15), are the subsets of the unified model equations shown in (16) and (17).

The highly nonlinear and dispersive models have been extended to include the effects of porous bottom. Hsiao *et al.* (2002) has used the model to investigate the effects of submerged breakwater. In studying the landslide-generated waves, Lynett and Liu (2002) has extended (16) and (17) by adding the terms involving the time derivatives of water depth. Lynett *et al.* (2002) has also developed a numerical algorithm for calculating the moving shoreline, which has been one of challenging issues in applying the depth-integrated equations to nearshore problems.

3. Energy Dissipation

In the previous sections all the wave theories have been developed based on the assumption that no energy dissipation occurs during the wave transformation process. However, in most coastal problems the effects of energy dissipation, such as bottom friction and wave breaking may become significant.

The mild-slope equation may be modified in a simple manner to accommodate these phenomena by including an energy dissipation function describing the rate of change of wave energy. The energy dissipation functions are usually defined empirically according to different dissipative processes (*e.g.,* Dalrymple *et al.* 1984). To consider wave breaking in the parabolic approximation of the mild-slope equation for spectral wave conditions it is possible to introduce a wave breaking term αA_{jl}, where A_{jl} represents the complex wave amplitude for the *j-th* wave frequency component and *l-th* component in direction and α is a dissipation coefficient that depends on the wave breaking model employed. For example, considering the breaking model by Thornton and Guza (1983) the dissipation coefficient is defined as

$$\alpha = \frac{3\sqrt{\pi}}{4}\frac{\overline{f}B^3}{\gamma^4 h^5}H_{rms}^5$$

where h is the local water depth, $\overline{f}$ is a representative wave frequency, and B and γ are empirical constants chosen to be 1 and 0.6, respectively.

In the following discussions, numerical results of a parabolic approximation model for spectral waves (OLUCA-SP, GIOC (2000)) and experimental data (Chawla *et al.* 1998) are presented. Regarding the wave breaking, the OLUCA-SP has the option of using several models: Thornton and Guza (1983), Battjes and Janssen (1978) and Rattanapitikon and Shibayama (1998).

Chawla *et al.* (1998) presented an experimental study of random directional waves breaking over a submerged circular shoal. Experiments were carried out in a wave basin 18.2 m long and 18.2 m wide. The circular shoal had a diameter of 5.2 m, a maximum height of 37 cm and was located on a flat bottom as shown in Figure 2. During the experiments, the water depth away from the shoal was kept at 40 cm and the water depth on the top of the shoal was 3 cm. Wave gauges were used to obtain a total of 126 measuring points around the shoal. In order to perform comparisons a longitudinal transect (A-A') and six transverse transects were considered, as shown in Figure 2. Four directional sea conditions were simulated with a TMA frequency spectrum (Bouws *et al.* 1985) and a directional spreading function (Borgman 1984). In the following only two of the four tests performed were chosen to demonstrate the capabilities of the parabolic model. The correspondent parameters of the tests selected are given in Table 1, in which H_{O_s} is the input significant wave height, T_p is the peak pe-

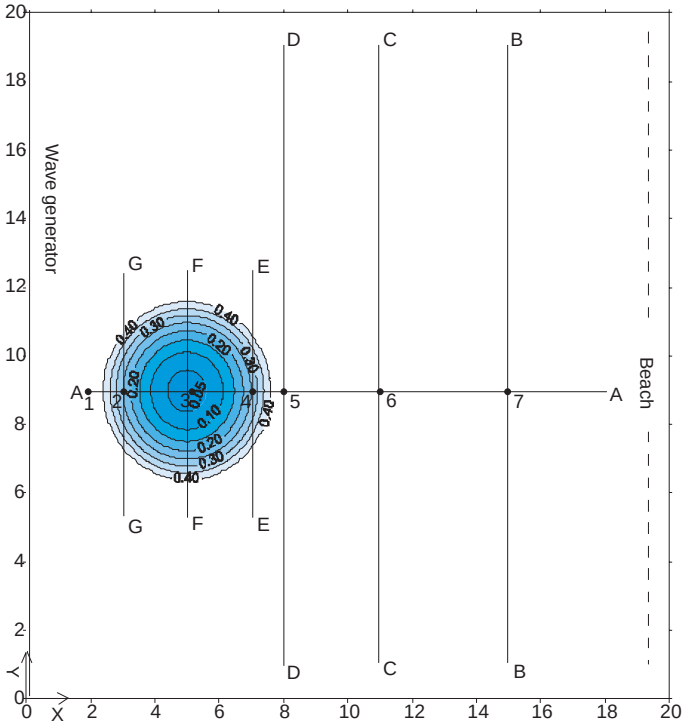

Fig. 2 Schematic view of experimental setup and gage transect locations, Chawla *et al.* (1998).

riod, θ_m is the mean wave direction, σ_m determines the width of the directional spreading and Γ is the width of the frequency spectrum.

Table 1. Parameters for spectral tests (Chawla *et al.* 1998)

Test	$H_{O_s}(m)$	$T_p(s)$	Γ	$\theta_m(°)$	$\sigma_m(°)$
3	0.0139	0.73	10	0	5
6	0.0249	0.71	10	0	20

The parabolic approximation model requires the incoming directional random sea at the offshore boundary as an input. The computational domain is discretized using a rid of 161 rows and 181 components, grid size being 10 cm by 10 cm. The incident spectra were discretized using 30 frequency and 30 directional components. For details on the computational procedure and algorithms see, GIOC (2000).

Figure 3 presents a plot of the free surface at a given instant obtained numerically using the OLUCA-SP and a wave breaking model by Thornton and Guza (1983) for Case 3 (see Table 1). The effects of the presence of the shoal are clearly visible since Case 3 corresponds to a narrow directional spread.

Assuming a Rayleigh wave height distribution, the significant wave heights for the data and the model can be obtained. Figure 4 gives the comparison of the normalized wave heights between the calculated values and the experimental data along different transects, for Case 6, which corresponds to a broader directional spread than Case 3. Wave heights have been normalized using the input significant wave height, H_{0s}. The comparison is quite good except near the top of the shoal where the numerical model slightly over-predicts the experimental data.

Figure 5 presents the comparisons for Case 6 along other

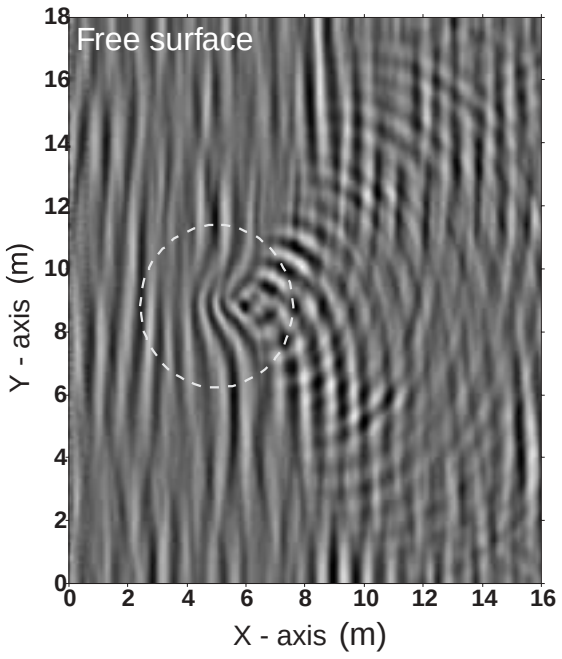

Fig. 3 Numerical simulation of the free surface elevation for Case 3 (narrow-directional spread)

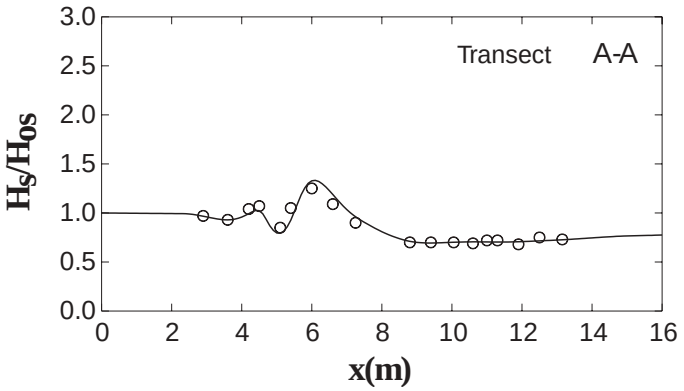

Fig. 4 Normalized significant wave heights along transect A-A for Case 6. Experimental data: o o o; numerical results (OLUCA-SP): —. Dissipation model: Thornton and Guza (1983) (B =1.0 and $\gamma = 0.6$).

transects. The numerical results (solid lines) show for all transects a large significant wave height at the side-walls due to the reflecting wall boundary condition. Clearly, the worst comparisons are obtained on the top of the shoal (F-F) where the focusing and the wave breaking take place. However, in general the comparisons are good in all transects.

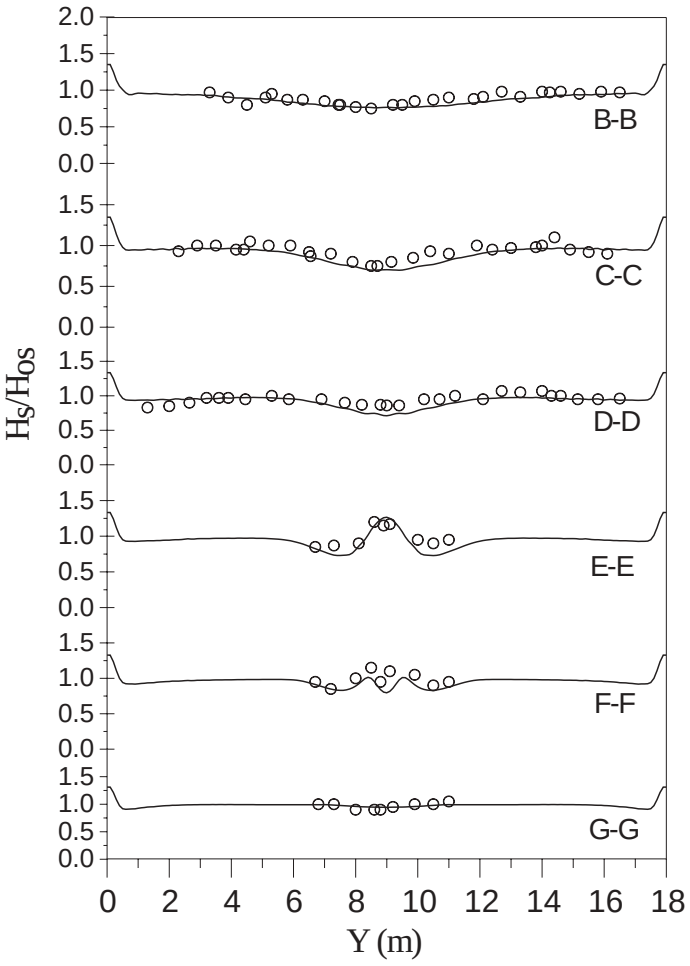

Fig. 5 Normalized significant wave heights along the transects shown in Figure 2 for Case 6 (Broad directional spread). Experimental data: o o o; numerical data (OLUCA-SP): —. Dissipation model: Thornton and Guza (1983) (B = 1.0 and $\gamma = 0.6$).

Figure 6 shows a comparison of calculated model spectra with data spectra on several locations along transect A-A for Case 3. Two different wave breaking models have been considered; Thornton and Guza (1983) and Battjes and Janssen (1978). As can be seen, the numerical model is able to give relatively good results. However, major disparities arise on the top of the shoal. At this position the model is very sensitive to the wave breaking model considered.

Similarly, in the numerical models based on Boussinesq-type equations, adding a new term to the depth-integrated momentum equation parameterizes the wave breaking process. While Zelt (1991), Karambas and Koutitas (1992) and Kennedy *et al.* (2000) used the eddy viscosity model, Brocchini *et al*. (1992) and Schäffer *et al*. (1993) employed a more complicated roller model based on the surface roller concept for spilling breakers. In the roller model the instantaneous roller thickness at each point and the orientation of the roller must be prescribed. Furthermore, in both approximations incipient breaking has to be determined making certain assumptions. By adjusting parameters associated with the breaking models, results of these models all showed very reasonable agreement with the respective laboratory data for free surface profiles. However, these models are unlikely to produce accurate solutions for the velocity field or to determine spatial distributions of the turbulent kinetic energy and therefore, more specific models on breaking waves are needed.

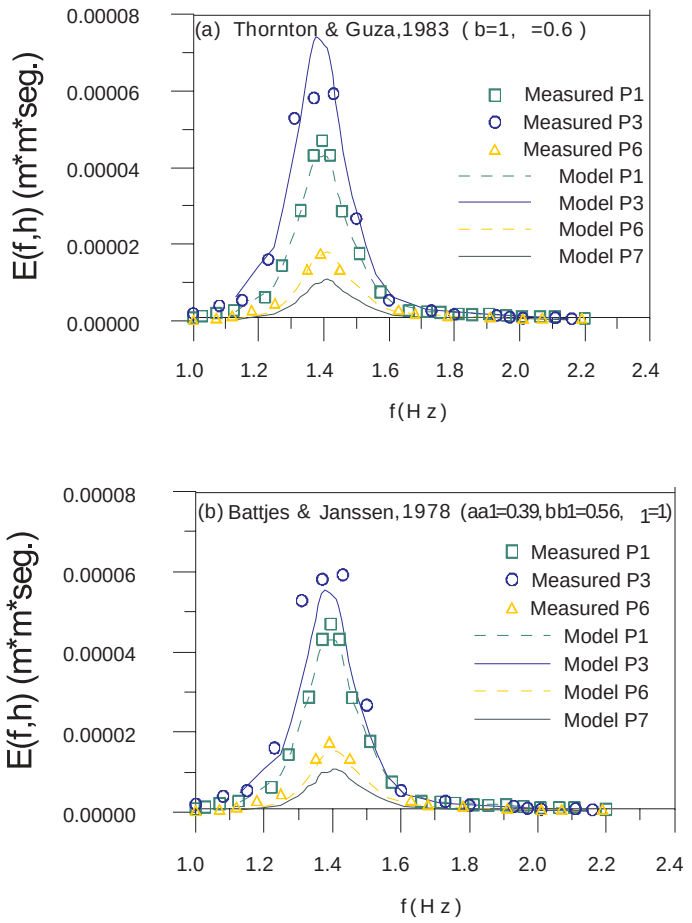

Fig. 6 Comparison of the frequency spectra for Case 3 (narrow-directional spread). P_i indicates the location of the points on transect A-A.

4. Reynolds Averaged Navier-Stokes (RANS) Equations Model for Breaking Waves

Numerical modeling of three-dimensional breaking waves is extremely difficult. Several challenging tasks must be overcome. First of all, one must be able to track accurately the free surface location during the wave breaking process so that the near surface dynamics is captured. Secondly, one must properly model the physics of turbulence production, transport and dissipation throughout the entire wave breaking process. Thirdly, one needs to overcome the huge demand in computational resources.

There have been some successful two-dimensional results. For instance, the marker and cell (MAC) method (e.g., Johnson *et al.* 1994) and the volume of fluid method (VOF) (*e.g.,* Ng and Kot 1992, Lin and Liu, 1998a) have been used to calculate two-dimensional breaking waves. The Reynolds Averaged Navier-Stokes (RANS) equations coupled with a second-order k-ε turbulence closure model have been shown to describe two-dimensional spilling and plunging breaking waves in surf zones (Lin and Liu 1998a,b). The Large Eddy Simulation (LES) approach has also been applied to two-dimensional breaking waves on a uniform slope (*e.g.,* Watanabe and Saeki 1999, Christensen and Deigaard 2001). The LES approach requires much finer grid resolution than the RANS approach, resulting in the very high demand on computational resources. However, very little research has been reported for simulating three-dimensional breaking waves. Miyata, *et al.* (1996) and Kawamura (1998) presented numerical models for three-dimensional ship waves by simulating a uniform free-surface flow passing a vertical cylinder. The dynamic process of quasi-steady state ship waves is quite different from that of the breaking waves in surf zone.

In this section the mathematical formulation and the associated numerical algorithm for the breaking wave model are discussed briefly. More detailed discussions can be found in Liu and Lin (1997) and Lin and Liu (1998 a, b). The breaking waves numerical model is based on the Reynolds Averaged Navier-Stokes (RANS) equations. For a turbulent flow, the velocity field and pressure field can be decomposed into two parts: the mean (ensemble average) velocity and pressure $\langle u_i \rangle$ and $\langle \mathrm{p} \rangle$, and the turbulent velocity and pressure u_i' and p'. Thus,

$$u_i = \langle u_i \rangle + u_i', \quad p = \langle p \rangle + p', \tag{18}$$

in which i = 1, 2, 3 for a three-dimensional flow. If the fluid is assumed incompressible, the mean flow field is governed by the Reynolds Averaged Navier-Stokes equations:

$$\frac{\partial \langle u_i \rangle}{\partial x_i} = 0, \tag{19}$$

$$\frac{\partial \langle u_i \rangle}{\partial t} + \langle u_j \rangle \frac{\partial \langle u_i \rangle}{\partial x_j} = -\frac{1}{\rho} \frac{\partial \langle p \rangle}{\partial x_i} + g_i + \frac{1}{\rho} \frac{\partial \langle \tau_{ij} \rangle}{\partial x_j} - \frac{\partial \langle u_i' u_j' \rangle}{\partial x_j}, \quad (20)$$

in which ρ is the density of the fluid, g_i the i-th component of the gravitational acceleration, and mean molecular stress tensor $\langle \tau_{ij} \rangle = 2\mu \langle \sigma_{ij} \rangle$ with μ being the molecular viscosity and $\langle \sigma_{ij} \rangle = \frac{1}{2} \left(\frac{\partial \langle u_i \rangle}{\partial x_j} + \frac{\partial \langle u_j \rangle}{\partial x_i} \right)$, the rate of strain tensor of the mean flow. In the momentum equation (20), the influence of the turbulent fluctuations on the mean flow field is represented by the Reynolds stress tensor $-\rho \langle u_i' u_j' \rangle$. Many second-order turbulence closure models have been developed for different applications, which have been summarized in a recent review article (Jaw and Chen 1998a,b). In the present model, the Reynolds stress, $-\rho \langle u_i' u_j' \rangle$, is expressed by a nonlinear algebraic stress model (Shih *et al*. 1996; Lin and Liu 1998a,b):

$$\begin{aligned} \rho \langle u_i' u_j' \rangle = {} & \frac{2}{3} \rho k \delta_{ij} - C_d \rho \frac{k^2}{\varepsilon} \left(\frac{\partial \langle u_i \rangle}{\partial x_j} + \frac{\partial \langle u_j \rangle}{\partial x_i} \right) \\ & - \rho \frac{k^3}{\varepsilon^2} \left[\begin{array}{l} C_1 \left(\frac{\partial \langle u_i \rangle}{\partial x_l} \frac{\partial \langle u_l \rangle}{\partial x_j} + \frac{\partial \langle u_j \rangle}{\partial x_l} \frac{\partial \langle u_l \rangle}{\partial x_i} - \frac{2}{3} \frac{\partial \langle u_l \rangle}{\partial x_k} \frac{\partial \langle u_k \rangle}{\partial x_l} \delta_{ij} \right) \\ + C_2 \left(\frac{\partial \langle u_i \rangle}{\partial x_k} \frac{\partial \langle u_j \rangle}{\partial x_k} - \frac{1}{3} \frac{\partial \langle u_l \rangle}{\partial x_k} \frac{\partial \langle u_l \rangle}{\partial x_k} \delta_{ij} \right) \\ + C_3 \left(\frac{\partial \langle u_k \rangle}{\partial x_i} \frac{\partial \langle u_k \rangle}{\partial x_j} - \frac{1}{3} \frac{\partial \langle u_l \rangle}{\partial x_k} \frac{\partial \langle u_l \rangle}{\partial x_k} \delta_{ij} \right) \end{array} \right] \end{aligned} \quad (21)$$

in which C_d, C_1, C_2, and C_3 are empirical coefficients, δ_{ij} the Kronecker delta, $k = \frac{1}{2} \langle u_i' u_i' \rangle$ the turbulent kinetic energy, and $\varepsilon = \nu \left\langle \left(\partial u_i' / \partial x_j \right)^2 \right\rangle$ the dissipation rate of turbulent kinetic energy, where $\nu = \mu / \rho$ is the molecular kinematic viscosity. It is noted that for the conventional eddy viscosity model $C_1 = C_2 = C_3 = 0$ in (21) and the eddy viscosity is then expressed as $\nu_t = C_d k^2/\varepsilon$. Compared with the conventional eddy viscosity model, the nonlinear Reynolds stress model (21) can be applied to general anisotropic turbulent flows.

The governing equations for k and ε are modeled as (Rodi 1980; Lin and Liu 1998a,b),

$$\frac{\partial k}{\partial t} + \langle u_j \rangle \frac{\partial k}{\partial x_j} = \frac{\partial}{\partial x_j} \left[\left(\frac{\nu_t}{\sigma_k} + \nu \right) \frac{\partial k}{\partial x_j} \right] - \langle u_i' u_j' \rangle \frac{\partial \langle u_i \rangle}{\partial x_j} - \varepsilon, \quad (22)$$

$$\begin{aligned} & \frac{\partial \varepsilon}{\partial t} + \langle u_j \rangle \frac{\partial \varepsilon}{\partial x_j} = \frac{\partial}{\partial x_j} \left[\left(\frac{\nu_t}{\sigma_\varepsilon} + \nu \right) \frac{\partial \varepsilon}{\partial x_j} \right] \\ & + C_{1\varepsilon} \frac{\varepsilon}{k} \nu_t \left(\frac{\partial \langle u_i \rangle}{\partial x_j} + \frac{\partial \langle u_j \rangle}{\partial x_i} \right) \frac{\partial \langle u_i \rangle}{\partial x_j} - C_{2\varepsilon} \frac{\varepsilon^2}{k}, \end{aligned} \quad (23)$$

in which σ_k, σ_ε, $C_{1\varepsilon}$, and $C_{2\varepsilon}$ are empirical coefficients. In the transport equation for the turbulent kinetic energy (22), the left-hand side term denotes the convection, while the first term on the right-hand side represents the diffusion. The second and the third term on the right-hand side of (22) are the production and the dissipation of turbulent kinetic energy, respectively.

The coefficients in equation (21) to (23) have been determined by performing many simple experiments and enforcing the physical realizability; the recommended values for these coefficients are (Rodi 1980; Lin and Liu 1998a,b):

$$\begin{aligned} & C_d = \frac{2}{3} \left(\frac{1}{7.4 + S_{\max}} \right), \; C_1 = \frac{1}{185.2 + D_{\max}^2} \\ & C_2 = -\frac{1}{58.5 + D_{\max}^2}, \quad C_3 = \frac{1}{370.4 + D_{\max}^2} \\ & C_{1\varepsilon} = 1.44, \quad C_{2\varepsilon} = 1.92, \quad \sigma_k = 1.0, \quad \sigma_\varepsilon = 1.3 \end{aligned} \quad (24)$$

where $S_{\max} = \frac{k}{\varepsilon} \max \left[\left| \frac{\partial \langle u_i \rangle}{\partial x_i} \right| \right]$ (repeated indices not summed) and $D_{\max} = \frac{k}{\varepsilon} \max \left[\left| \frac{\partial \langle u_i \rangle}{\partial x_j} \right| \right]$.

Appropriate boundary conditions need to be specified. For the mean flow field, the no-slip boundary condition is imposed on the solid boundary, and the zero-stress condition is required on the mean free surface by neglecting the effect of airflow. For the turbulent field, near the solid boundary, the log-law distribution of mean tangential velocity in the turbulent boundary layer is applied so that the values of k and ε can be expressed as functions of distance from the boundary and the mean tangential velocity outside of the viscous sublayer. On the free surface, the zero-gradient boundary conditions are imposed for both k and ε, i.e., $\partial k / \partial n = \partial \varepsilon / \partial n = 0$. A low level of k for the initial and inflow boundary conditions is assumed. The justification for this approximation can be found in Lin and Liu (1998a,b).

In the numerical model, the RANS equations are solved by the finite difference two-step projection method (Chorin, 1968). The forward time difference method is used to discretize the time derivative. The convection terms are discretized by the combination of central difference method and upwind method. The central difference method is employed to discretize the pressure gradient terms and stress gradient terms. The VOF method is used to track the free- surface (Hirt and Nichols 1981). The transport equations for k and ε are solved with the similar method used in solving the momentum equations. The detailed information can be found in Kothe *et al.* (1991), Lin and Liu (1997), and Lin and Liu (1998a,b).

The mathematical model described above has been verified by comparing numerical results with either experimental data or analytical solutions. For non-breaking waves, numerical models can accurately generate and propagate solitary waves as well as periodic waves (Liu and Lin 1997, Lin *et al*. 1998). The numerical model can also simulate the overturning of a surface jet as the initial phase of the plunging wave breaking processes (Lin and Liu 1998b). For both spilling and plunging breaking waves on a

beach the numerical results have been verified by laboratory data carefully performed by Ting and Kirby (1994, 1995). The detailed descriptions of the numerical results and their comparison with experimental data can be found in Liu and Lin (1997) and Lin and Liu (1998a,b). The overall agreement between numerical solutions and experimental data was very good. Although they are not shown here, the numerical results also have been used to explain the generation and transport of turbulence and vorticity throughout the wave breaking process. The vertical profiles of the eddy viscosity are obtained through out the surf zone. The surf similarity has been observed. Moreover, the model has also been used to demonstrate the different diffusion processes of pollutant release inside and outside of the surf zone (Lin and Liu 1998b).

More recently, the breaking wave model has been extended to investigate the interaction between breaking wave and coastal structures (Liu *et al.* 1999, Liu *et al*. 2000). These structures could be either surface piercing or totally submerged. The dynamic pressure distribution on the surface of the structure can be calculated and hence the wave forces. The model has been validated by several sets of experimental data (Sakakiyama and Liu 2001). Some of these experiments were performed at Cornell University and the experimental data were taken by the Particle Image Velocimetry (PIV) (Chang *et al.* 2001). More recently, the numerical model has been expanded to include the capability of describing free-surface flows in porous media. The model has been applied to calculate the runup and the overtop rate on a caisson breakwater protected by armor layers (Hsu *et al*. 2002).

Figure 7 shows the comparison between the numerical results and experimental data for the free surface evolution of a spilling breaker on an impermeable plane beach. The experimental setup has been described in Losada *et al.* (2000). The numerical model is able to reproduce the transient evolution of the breaking wave only with minor discrepancies.

In Figure 8 the horizontal velocity, u, and the vertical velocity, v, at gauge 17 are shown. Comparisons between numerical and experimental results are quite good. However, the horizontal velocity is slightly under-predicted by the numerical model at the different elevations considered. The vertical velocity is also underpredicted, especially close to the free surface.

Finally, in order to show the model capabilities to analyse wave and structure interaction, Figure 9 presents a numerical simulation of the velocity field in a rubble mound structure with a screen. Vectors show the flow under wave action in the vicinity and inside the core and secondary layers. Results correspond to the numerical simulation of a 1:18.4 scale model of Principe de Asturias breakwater in Gijon (Spain). The breakwater is built of a core made of 14.2 kg blocks and an armour layer of 19.3 blocks.

5. Concluding Remarks

Even though the computing power is rapidly increasing and that we are getting closer to be able to solve Navier-Stokes equations in a relatively large domain, wave propagation modeling is still dependent on several alternative mathematical formulations in order to simulate complex wave conditions in practical coastal engineering problems. In the last ten years tremendous efforts have been focused on the development of unified mathematical models describing wave propagation from deep to shallow waters. As a result, today several depth-integrated 2-D models for highly nonlinear and dispersive waves are available. Many aspects of

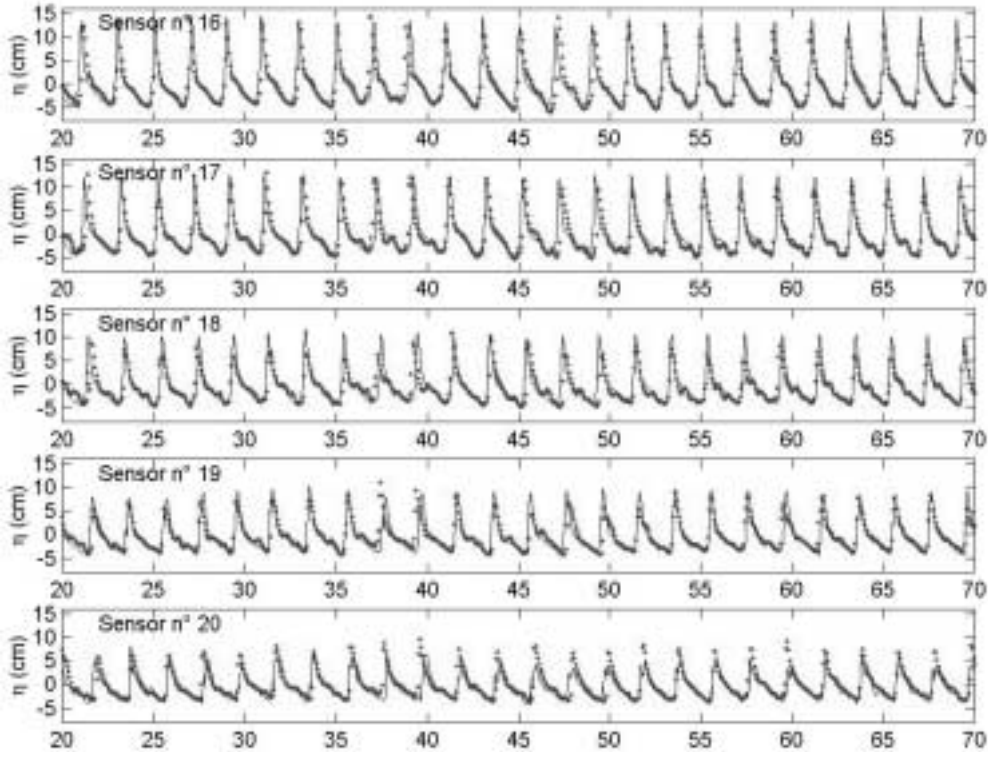

Fig. 7 Free surface evolution of a spilling breaker on an impermeable plane beach. Experimental data (-) and numerical results (···). Wave breaking starts at gauge 16.

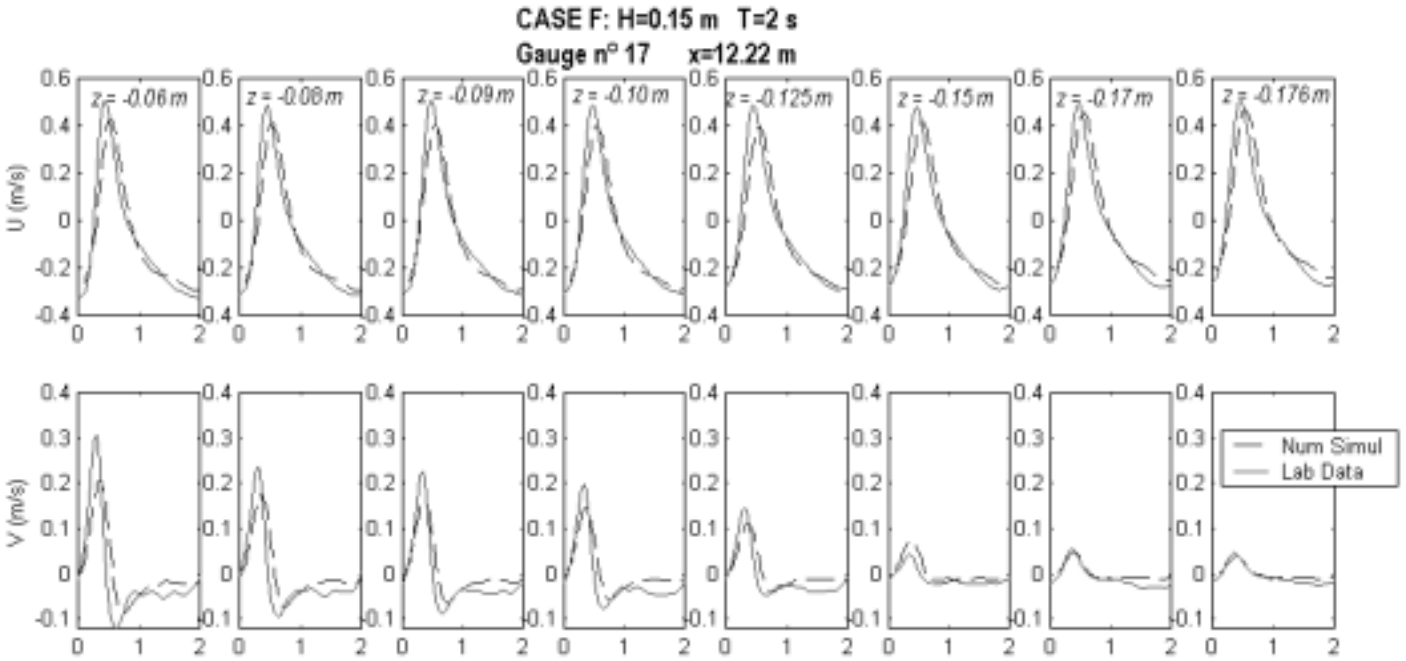

Fig. 8 Comparisons for horizontal and vertical velocities for previous case. Lab (solid line) and numerical model (---). SWL at z=0.

these models have been tested satisfactorily comparing numerical results with experimental field and laboratory data. At the present moment, if the model equations are truncated at $O(\mu^2)$, the model equations are adequate up to $kh \approx 3$. In principle, the higher frequency dispersive effects can always be included in the model equations by adding the higher terms in μ^2, resulting in higher spatial and temporal derivative terms. These higher derivatives terms create numerical difficulties as well as uncertainties in boundary conditions. Alternative approach must be taken if the unified models are to be applied to practical coastal engineering problems.

Our experience and ability of modeling wave breaking and wave and structure interaction have been improved considerably with the development of numerical models based on the Reynolds Averaged Navier Stokes equations. Today it is possible to analyze several dynamic processes in wave and structure interaction, such as wave dissipation and wave overtopping, only possible by means of physical models in the past. However, the development of these models is still at an early stage. The development of 3-D models, the search for adequate turbulence models, the optimiza-

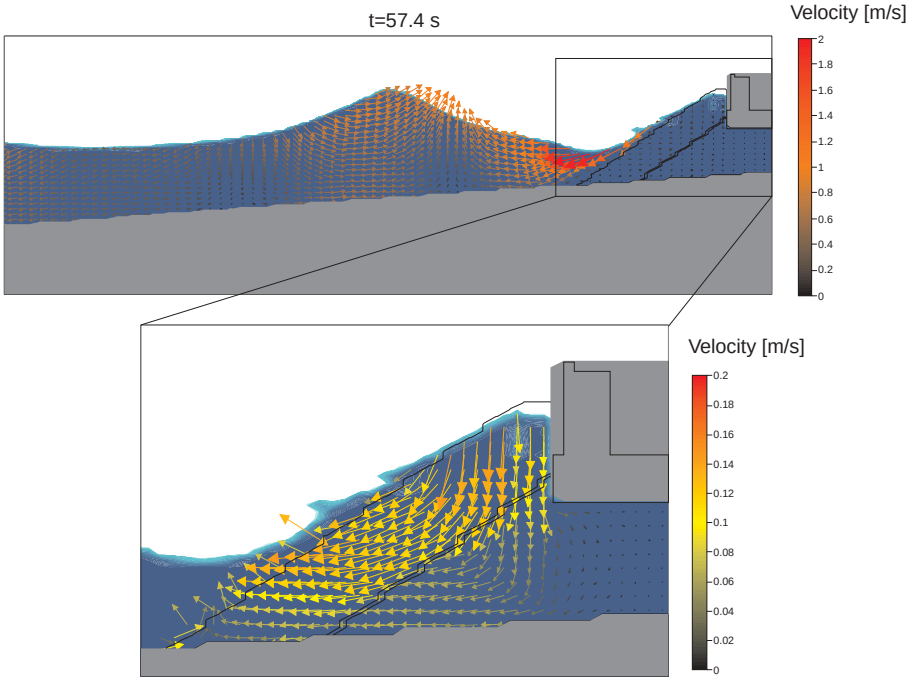

Fig. 9 Numerical description of the flow induced by a breaking wave approaching a composite breakwater.

tion of the numerical algorithms in order to reduce computational costs are some of the issues that are still to be addressed in order to improve model capabilities.

One of the future research challenges is to integrate the 2D depth-integrated model with the 3D RANS model. The 3D RANS is applied locally where either the breaking occurs or the wave-structure interaction is important. The 3D RANS results can either be integrated or be parameterized so that they are used in the 2D depth-integrated model. Alternatively, these two types of models can be coupled directly and solved simultaneously.

Acknowledgements

P. L.-F. Liu would like to acknowledge the financial supports received from National Science Foundation, Office of Naval Research, Army Research Office and Sea Grant Program. I.J. Losada is indebted to the Spanish Comision Interministerial de Ciencia y Tecnologia for the funding provided in project MAR99-0653.

References

BATTJES, J.A. and JANSSEN, J.P.F.M. 1978. 'Energy loss and set-up due to breaking of random waves.' *Proceedings of the 16th International Coastal Engineering Conference, ASCE*, 569-587.

BERKHOFF, J. C. W. 1972. 'Computation of combined refraction and diffraction', *Proceedings of the 13th International Coastal Engineering Conference, ASCE*, 471-490.

BERKHOFF, J. C. W. 1976. *Mathematical models for simple harmonic linear water waves; wave refraction and diffraction.* PhD thesis, Delft Technical University of Technology.

BORGMAN, L.E. 1984. 'Directional spectrum estimation for S_{xy} gages.' *Technical Report. CERC, Vicksburg, MS.*

BOUWS, E., GUNTHER, H., ROSENTHAL, W. and VINCENT, C. 1985. 'Similarity of the wind wave spectrum in finite depth water.' *J. Geophys. Res.,* 90, 975-986.

BROCCHINI, M., DRAGO, M. and IVOENITTI, L. 1992. 'The modeling of short waves in shallow water: Comparison of numerical model based on Boussinesq and Serre equations.' *Proc. 23rd Intnl. Conf. Coastal Engng*. ASCE. 76-88.

CHANG, K.-A., HSU, T.-J., and LIU, P. L.-F. 2001. 'Vortex generation and evolution in water waves propagating over a submerged rectangular obstacle. Part I. solitary waves', *Coastal Engrg*., 44, 13-36.

CHAWLA, A., ÖZKAN, H. T. and KIRBY, J.T. 1998. 'Spectral model for wave transformation and breaking over irregular bathymetry*', J. Water., Port, Coastal and Ocean Eng*., 124 (4), pp. 189-198.

CHEN, Q., MADSEN, P. A., SCHAFFER, H. A. and BASCO, D. R., 1998 'Wave-current interaction based on an enhanced Boussinesq approach', *Coastal Engng*., **33**, 11-39.

CHEN, Y. and LIU, P. L.-F. 1994 'A Pseudo-Spectral Approach for Scattering of Water Waves', *Proc. Roy. Soc. London*, **A, 445**, 619-636.

CHEN, Y. and LIU, P. L.-F. 1995 'Modified Boussinesq equations and associated parabolic models for water wave propagation,' *J. Fluid Mech*., **288**, 351-381.

CHORIN, A.J. 1968 'Numerical solution of the Navier-Stokes equations.' *Math. Comput*. **22**, 745-762.

CHRISTENSEN, E.D. and DEIGAARD, R. 2001 'Large scale simulation of breaking waves', *Coastal Engrg*., **42(1),** 53-86.

DALRYMPLE, R.A., KIRBY, R.T. and HWANG, P.A. 1984. 'Wave diffraction due to area of energy dissipation.' *J. Waterway, Port, Coastal, and Ocean Engineering*, ASCE., **110** (1), 67-79.

ECKART, C. 1952 'The propagation of gravity waves from deep to shallow water'. Circular 20, *National Bureau of Standards*, 165-173.

ELGAR, S. and GUZA, R. T. 1985 'Shoaling gravity waves: comparisons between field observations, linear theory and a nonlinear model', *J. Fluid Mech*., **158**, 47-70.

GIOC 2000. 'OLUCA-SP Users guide and reference manual, version 2.0.' Ocean & Coastal Research Group. University of Cantabria, Spain.

GORING, D. G. 1978 *Tsunamis - the propagation of long waves onto a shelf*, Ph.D. dissertation, California Institute of Technology, Pasadena, CA.

HIRT, C.W. and NICHOLS, B.D. 1981 'Volume of fluid (VOF) method for dynamics of free boundaries.' *J. Comput. Phys*. **39**, 201-225.

HSIAO, S.-C., LIU, P. L.-F. and CHEN, Y. 2001 'Nonlinear Water Waves propagating Over a Permeable Bed', *Proc. Roy. Soc. London,* A (in press).

HSU, T.-J., SAKAKIYAMA, T. and LIU, P. L.-F. 2002 'Validation of a Model for Wave-Structure Interactions', *Coastal Engrg* (in press).

JAW, S.Y. and CHEN, C.J. 1998a 'Present status of second-order closure turbulence model. I: overview.' *J. Engineering Mechanics,* **124,** 485-501.

JAW, S.Y. and CHEN, C.J. 1998b 'Present status of second-order closure turbulence models. II: application.' *J. Engineering Mechanics,* **124,** 502-512.

JOHNSON, D.B., RAAD, P.E. and CHEN, S. 1994, 'Simulation of impacts of fluid free surface with solid boundary,' *Int. J. Numer. Meth. Fluids,* **19,** 153-174.

KARAMBAS, Th. V. and KOUTITAS, C. 1992. 'A breaking wave propagation model based on the Boussinesq equations.' *Coastal Engng*, **18**, 1-19.

KAWAMURA, T. 1998 *Numerical simulation of 3D turbulent free-surface flows*, International Research Center for Computational Hydrodynamics (ICCH), Denmark.

KENNEDY, A.B., CHEN, Q., KIRBY, J.T. and DALRYMPLE, R.A. 2000. 'Boussinesq modeling of wave transformation, breaking and runup, I: 1D.' *J. Waterway, Port, Coastal, and Ocean Engineering*, ASCE, **126** (1), 39-48.

KIRBY J.T. and DALRYMPLE, R.A..1983. 'A parabolic equation for the combined refracion-diffraction of Stokes waves by mildly varying topography.' *J. Fluid Mech*., **136,** 543-566.

KOTHE, D.B., MJOLSNESS, R.C. and TORREY, M.D. 1991 'RIPPLE: a computer program for incompressible flows with free surfaces.' Los Alamos National Laboratory, LA-12007-MS.

LIN, P. and LIU, P. L.-F. 1998a 'A Numerical Study of Breaking

Waves in the Surf Zone', *J. Fluid Mech.*, **359**, 239-264.

LIN, P. and LIU, P. L.-F. 1998b 'Turbulence Transport, Vorticity Dynamics, and Solute Mixing Under Plunging Breaking Waves in Surf Zone,' *J. Geophys. Res.*, **103**, 15677-15694.

LIN, P., CHANG, K.-A., and LIU, P. L.-F. 1999 'Runup and rundown of solitary waves on sloping beaches', *J. Waterway, Port, Coastal and Ocean Engrg*., ASCE, **125 (5),** 247-255.

LIU, P. L.-F. 1990 'Wave transformation', in *the Sea*, **9,** 27-63.

LIU, P. L.-F. 1994 'Model equations for wave propagation from deep to shallow water', in *Advances in Coastal and Ocean Engineering,* **1,** 125-158.

LIU, P. L.-F. and TSAY, T.K. 1983 'On weak reflection of water waves,' *J. Fluid Mechanics*, **131**, 59-71.

LIU, P. L.-F. and TSAY, T-K. 1984 'Refraction-Diffraction Model for Weakly Nonlinear Water Waves," *J. Fluid Mech.*, **141**, 265-74.

LIU, P. L.-F. and LIN, P. 1997 'A numerical model for breaking wave: the volume of fluid method.' *Research Rep. CACR-97-02*. Center for Applied Coastal Research, Ocean Eng. Lab., Univ. of Delaware, Newark, Delaware 19716.

LIU, P. L.-F., YOON, S. B. and KIRBY, J. T. 1985 'Nonlinear refraction-diffraction of waves in shallow water', *J. Fluid Mech.*, **153**, 185-201.

LIU, P. L.-F., CHO, Y.-S., BRIGGS, M. J., KANOGLU, U., and SYNOLAKIS, C. E., 1995 'Runup of Solitary Waves on a Circular Island,' *J. Fluid Mech.*, **302**, 259-285.

LIU, P. L.-F., LIN, P., CHANG, K.-A., and SAKAKIYAMA, T. 1999 'Wave interaction with porous structures' , *J. Waterway, Port, Coastal and Ocean Engrg*., ASCE, **125 (6),** 322-330.

LIU P.L.-F, LIN, P., HSU, T., CHANG, K., LOSADA, I.J., VIDAL, C. and SAKAKIYAMA, T. 2000. 'A Reynolds averaged Navier-Stokes equation model for nonlinear water wave and structure interactions.' *Proceedings Coastal Structures 99*. A.A. Balkema. Rotterdam. pp. 169-174.

LOSADA, I.J., LARA, J.L and LOSADA, M.A. 2000. 'Experimental study on the influence of bottom permeability on wave breaking and associated processes' *Proc. 27th Intnl. Conf. Coastal Engng*. ASCE. 706-719.

LYNETT, P. and LIU, P. L.-F. 2002 'A numerical study of submarine landslide generated waves and runups', *Proc. Roy. Soc. London*, A (in press).

LYNETT, P., WU, T.-R. and LIU, P. L.-F. 2002 'Modeling wave runup with depth-integrated equations', *Coastal Engrg,* (in press).

MADSEN, P. A., MURRAY, R. and SORENSEN, O. R. 1991 'A new form of the Boussinesq equations with improved linear dispersion characteristics*',* *Coastal Engng*, **15**, 371-388.

MADSEN, P. A., SORENSEN, O. R. and SCHAFFER, H. A. 1997 'Surf zone dynamics simulated by a Boussinesq-type model. Part II. Surf beat and swash oscillation for wave groups and irregular waves', *Coastal Engng*, **32**, 189-319.

MEI, C. C. and LIU, P. L.-F. 1993 'Surface waves and coastal dynamics', *Annu. Rev. Fluid Mech*., **25**, 215-240.

MIYATA, H., KANAI, A., KAWAMURA, T. and PARK, J-C. 1996 'Numerical simulation of three-dimensional breaking waves', *J. Mar. Sci. Technol*., **1**, 183-197.

NG, C. O. and KOT, S.C. 1992 'Computations of water impact on a two-dimensional flat-bottom body with a volume of fluid method', *Ocean Eng.* **19**, 377-393.

NWOGU, O. 1993 'An alternative form of the Boussinesq equations for nearshore wave propagation', *J. Waterway. Port, Coast. Ocean Engng, ASCE*, **119**, 618-638.

PEREGRINE, D. H. 1967 'Long waves on a beach' *J. Fluid Mech.*, **27**, 815-882.

RATTANAPITIKON, W. and SHIBAYAMA, T. 1998. 'Energy dissipation model for regular and irregular breaking waves.' *Coastal Eng. J*., **40 (4),** 327-346.

RODI, W. 1980. 'Turbulence models and their application in hydraulics - a state-of-the-art review.' *IAHR Publication*.

SAKAKIYAMA, T. and LIU, P. L.-F. 2001 'Laboratory experiments for wave motions and turbulence flows in front of a breakwater', *Coastal Engrg*, **44,** 117-139.

SCHÄFFER, H.A., MADSEN, P.A. and DEIGAARD, R.A. 1993. ' A Boussinesq model for waves breaking in shallow water.' *Coastal Engng*, **20**, 185-202.

SHIH, T.-H., ZHU, J. and LUMLEY, J.L. 1996. 'Calculation of wall-bounded complex flows and free shear flows.' *Intl J. Numer. Meth. Fluids,* **23**, 1133-1144.

SMITH, T. and SPRINKS, R. 1975. 'Scattering of surface waves by a conical island.' *J. Fluid Mech.*, **72**, 373-384.

THORNTON, E.B. and GUZA, R.T. 1983. 'Transformation of wave height distribution.' *J. Geophys. Res.,* **88 (C10),** 5925-5938.

TING, F.C.K. and KIRBY, J.T. 1994, 'Observation of undertow and turbulence in a laboratory surf zone.' *Coastal Engng,* **24**, 51-80.

TING, F.C.K. and KIRBY, J.T. 1995, 'Dynamics of surf-zone turbulence in a strong plunging breaker.' *Coastal Engng,* **24**, 177-204.

TSAY, T.-K. and LIU, P.L.-F. 1982. 'Numerical solution of water-wave refraction and diffraction problems in the parabolic approximation. *J. Geophys. Res.*, **87 (C10),** 7932-7940.

WATANABE, Y. and SAEKI, H., 1999 'Three-dimensional large eddy simulation of breaking waves', *Coastal Engrg. J.*, **3&4,** 282-301.

WEI, G., KIRBY, J. T., GRILLI, S. T. and SUBRAMANYA, R. 1995 'A fully nonlinear Boussinesq model for surface waves. Part I Highly nonlinear unsteady waves,' *J. Fluid Mech*., **294**, 71-92.

WITTING, J. M. 1984 'A unified model for the evolution of nonlinear water waves', *J. Comp. Phys.,* **56**, 203-236.

ZELT, J. L. 1991 'The run-up of nonbreaking and breaking solitary waves*',* *Coastal Engng*, **15**, 205-246.